Short Papers

Scattering at a Nonchiral–Chiral Interface in a Coaxial Waveguide

Zhongxiang Shen and Robert H. MacPhie

***Abstract*— A formally exact full-wave solution is presented for the problem of scattering at a nonchiral–chiral interface in a coaxial waveguide. The field components for the axisymmetric modes in a coaxial chirowaveguide are initially obtained. A new orthogonality relation for the modes is then proposed and used to find expansion coefficients for the electromagnetic fields in the coaxial chirowaveguide. The scattering matrix for the nonchiral–chiral dielectric discontinuity in a coaxial waveguide is finally derived by enforcing the continuity conditions of the tangential field components across the interface. Numerical results for the reflection and transmission coefficients at the nonchiral–chiral interface in a coaxial waveguide are presented.**

***Index Terms*—Chiral material, mode-matching method, waveguide discontinuity.**

I. Introduction

The notion of electromagnetic chirality, also known as optical activity in the optical regime, has been recognized since the beginning of the Nineteenth century. In the past few years, a considerable amount of work was carried out to investigate its potential application to problems in radiation and scattering and propagation in unbounded and bounded media [1], [2]. This paper deals with the theoretical analysis of reflection and transmission at a nonchiral–chiral interface in a coaxial waveguide. Fig. 1 shows the side view of the structure of the problem considered, whose analysis mainly involves the characterization of a dielectric step discontinuity (nonchiral–chiral interface) in a coaxial waveguide. The motivation behind this study is the possibility of determining material parameters of chiral media using a coaxial line. Using the coaxial line (rather than the parallel-plate waveguide [3]) is more attainable from the point of view of measurement.

II. Modes in a Coaxial Chirowaveguide

This section gives the electromagnetic-field expressions for axisymmetric modes in a coaxial chirowaveguide. A new orthogonality relation for these modes is also proposed.

A. Field Components

For time-harmonic electromagnetic fields with $\exp(j\omega t)$ dependence, the basic constitutive relations for describing a chiral medium are of the form

$$\vec{D} = \epsilon\vec{E} - j\xi\vec{B} \tag{1a}$$

$$\vec{H} = -j\xi\vec{E} + \vec{B}/\mu \tag{1b}$$

where ϵ, μ, and ξ are the permittivity, permeability, and chirality admittance of a chiral medium, respectively. A chirowaveguide consists of a conventional cylindrical waveguide filled with a homogeneous chiral medium characterized by (1). The theory of chirowaveguides and propagation characteristics of their modes were investigated in detail in the literature [2]–[5]. For the sake of completeness, we summarize some of these results here. The transverse-field components in chirowaveguides are related to the longitudinal components by the following relations:

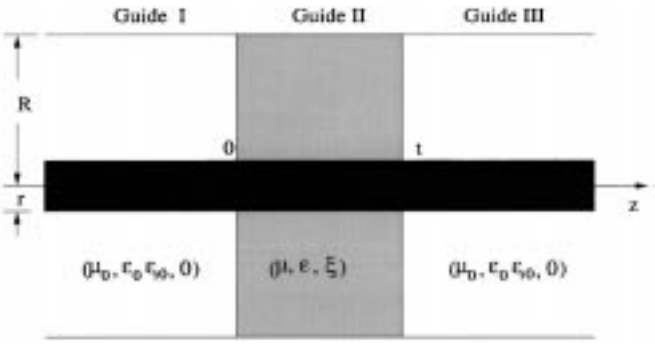

Fig. 1. Geometry of the structure considered.

$$\vec{e}_t = a\hat{z} \times \nabla_t e_z - jb\nabla_t e_z + jc\hat{z} \times \nabla_t h_z + d\nabla_t h_z \tag{2a}$$

$$\vec{h}_t = -j\frac{c}{\eta_c^2}\hat{z} \times \nabla_t e_z - \frac{d}{\eta_c^2}\nabla_t e_z + a\hat{z} \times \nabla_t h_z - jb\nabla_t h_z \tag{2b}$$

where

$$\begin{aligned} a &= \omega\mu\xi(k^2+\beta^2)/\Delta, \\ b &= \beta(2\omega^2\mu^2\xi^2 + k^2 - \beta^2)/\Delta \\ c &= \omega\mu(k^2-\beta^2)/\Delta \\ d &= 2\beta\omega^2\mu^2\xi/\Delta \\ k^2 &= \omega^2\mu\epsilon \\ \Delta &= \beta^4 - 2\beta^2(2\omega^2\mu^2\xi^2 + k^2) + k^4 \\ \eta_c &= \sqrt{\mu/(\epsilon+\mu\xi^2)}. \end{aligned}$$

The longitudinal field components e_z and h_z can be expressed by

$$e_z = (P^+)^2U^+ + (P^-)^2U^- \tag{3a}$$

$$h_z = j[(P^+)^2U^+ - (P^-)^2U^-]/\eta_c \tag{3b}$$

where

$$(P^\pm)^2 = (k^\pm)^2 - \beta^2,\ k^\pm = \pm\omega\mu\xi + \sqrt{k^2 + \omega^2\mu^2\xi^2}$$

and U^+ and U^- are solutions of Helmholtz equation [4].

Now our attention turns to the electromagnetic-field expressions and propagation constants of axisymmetric modes in a coaxial chirowaveguide. It has been shown [2]–[5] that a chirowaveguide is unable to support individual TE, TM, or TEM modes, that is to say, all the modes existing in a chirowaveguide are hybrid. For the problem considered in this paper, only axisymmetric modes can be excited in both the conventional coaxial line (Guide I in Fig. 1) and the coaxial chirowaveguide (Guide II) due to the symmetry of the structure and the incident TEM mode in Guide I. For the axisymmetric modes in a coaxial chirowaveguide with r and R being its inner and outer radii, respectively, use of (2) and (3) is made to derive the following

Manuscript received March 12, 1996; revised April 7, 1998.

The authors are with the Department of Electrical and Computer Engineering, University of Waterloo, Waterloo, Ont., Canada N2L 3G1.

Publisher Item Identifier S 0018-9480(98)04949-7.

field-component expressions:

$$e_z = P^+[J_0(P^+\rho) + Y_0(P^+\rho)B^+] + P^-[J_0(P^-\rho)A^- + Y_0(P^-\rho)B^-] \quad (4a)$$

$$h_z = jP^+[J_0(P^+\rho) + Y_0(P^+\rho)B^+]/\eta_c - jP^-[J_0(P^-\rho)A^- + Y_0(P^-\rho)B^-]/\eta_c \quad (4b)$$

$$e_\rho = -j\beta[J_0'(P^+\rho) + Y_0'(P^+\rho)B^+ + J_0'(P^-\rho)A^- + Y_0'(P^-\rho)B^-] \quad (4c)$$

$$h_\rho = \beta[J_0'(P^+\rho) + Y_0'(P^+\rho)B^+ - J_0'(P^-\rho)A^- - Y_0'(P^-\rho)B^-]/\eta_c \quad (4d)$$

$$e_\phi = -k^+[J_0'(P^+\rho) + Y_0'(P^+\rho)B^+] + k^-[J_0'(P^-\rho)A^- + Y_0'(P^-\rho)B^-] \quad (4e)$$

$$h_\phi = k^+[J_0'(P^+\rho) + Y_0'(P^+\rho)B^+]/(j\eta_c) + k^-[J_0'(P^-\rho)A^- + Y_0'(P^-\rho)B^-]/(j\eta_c) \quad (4f)$$

where J_0 and Y_0 are the zeroth-order Bessel functions of the first and second kind, respectively; the prime denotes the derivative of Bessel functions with respect to their entire argument. From (4) and the condition that tangential electric-field components must be zero on the conductor surfaces, we can easily obtain the characteristic equation for the propagation constant β of axisymmetric modes in a coaxial chirowaveguide. It should be pointed out that for $(P^-)^2 < 0$, $J_0(P^-\rho)$ and $Y_0(P^-\rho)$ in (4) are, respectively, replaced by $I_0(|P^-|\rho)$ and $K_0(|P^-|\rho)$ with I_0 and K_0 being the first and second kind of modified Bessel functions of order 0. After finding the propagation constant for a specific mode, the corresponding expressions for A^-, B^-, and B^+ can be readily found.

B. Mode Orthogonality

It is well known that the mode orthogonality for a conventional metallic waveguide filled with homogeneous nonchiral materials has the form [6]

$$\int_s \vec{e}_{tn} \cdot \vec{e}_{tm}\, ds = \int_s \vec{h}_{tn} \cdot \vec{h}_{tm}\, ds = 0, \qquad \text{for } n \neq m \quad (5)$$

where the subscript t denotes the tangential component. However, for a waveguide filled with inhomogeneous nonchiral materials, (5) does not hold true in a general sense; a more general mode orthogonality exists [6] as follows:

$$\int_s \vec{e}_{tn} \times \vec{h}_{tm} \cdot \hat{z}\, ds = 0, \qquad \text{for } n \neq m \quad (6a)$$

which, in the cylindrical coordinates (ρ, ϕ), will reduce to

$$\int_s (e_{\rho n} h_{\phi m} - e_{\phi n} h_{\rho m})\, ds = 0, \qquad \text{for } n \neq m. \quad (6b)$$

Relation (6) is very useful for the analysis of waveguide discontinuities involving inhomogeneous dielectrics. For chirowaveguides, Engheta and Pelet [7] derived an orthogonality relation for their modes as follows:

$$\int_s (\vec{e}_n \times \vec{h}_m - \vec{e}_m \times \vec{h}_n) \cdot \hat{z}\, ds = 0 \quad (7)$$

which holds true for waveguides filled with both lossless and lossy chiral materials. Unfortunately, relation (7) is of no use for modal expansions. It is shown in [8] that another similar relation involving complex conjugates for lossless chirowaveguides is not suitable for modal expansions in the power sense either. In the following, we introduce a new orthogonality for the axisymmetric modes in a coaxial chirowaveguide. Recalling the field expressions in (4) and employing the technique of reversing the propagation direction used in [6], one can show that the axisymmetric modes in the coaxial chirowaveguide satisfy the following orthogonal relation:

$$\int_s (e_{\rho n} h_{\phi m} + h_{\rho n} e_{\phi m})\, ds = 0, \qquad \text{for } n \neq m. \quad (8)$$

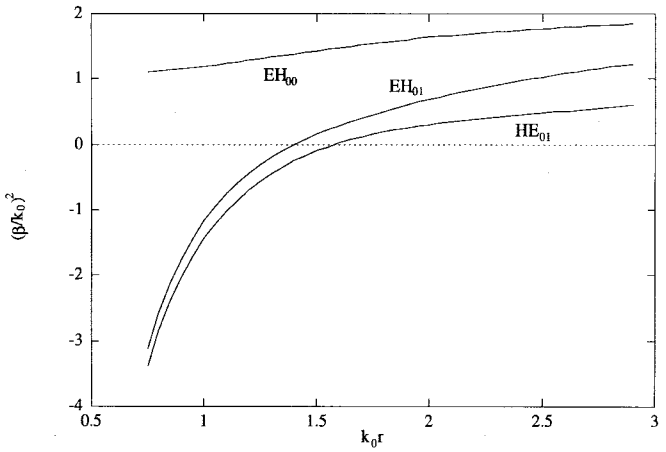

Fig. 2. Dispersion diagram of the first three axisymmetric modes in a coaxial chirowaveguide ($R = 3r$, $\epsilon_r = \mu_r = 1$, $\xi = 1mS$).

This orthogonality relation will be used in Section III to express the electromagnetic-field components by the sum of their modal functions and to derive the scattering matrix of a nonchiral–chiral dielectric discontinuity in a coaxial waveguide.

III. The Scattering Matrix

The structure of the problem in which we are interested is shown in Fig. 1, where the nonchiral–chiral interface is assumed to be at the plane of $z = 0$. For the conventional coaxial waveguide (Fig. 1, Guide I), the transverse components of electromagnetic fields can be expressed by

$$\vec{E}_{1t} = \sum_{m=1}^{N_1} [A_{1m}^i \exp(-j\beta_{1m}z) + A_{1m}^r \exp(j\beta_{1m}z)]\vec{e}_{1tm} \quad (9a)$$

$$\vec{H}_{1t} = \sum_{m=1}^{N_1} [A_{1m}^i \exp(-j\beta_{1m}z) - A_{1m}^r \exp(j\beta_{1m}z)]Y_{1m}\hat{z} \times \vec{e}_{1tm} \quad (9b)$$

where expressions for the normalized electric field $\vec{e}_{1tm}$ are available in [9]; Y_{1m} and β_{1m} are the mode admittance and propagation constant, respectively, and A_{1m}^i and A_{1m}^r are the incident and reflected modal amplitudes of mode m.

The transverse-field components in the coaxial chirowaveguide (Fig. 1, Guide II) are of the form

$$E_{2\rho} = \sum_{n=1}^{N_2} [A_{2n}^r \exp(-j\beta_{2n}z) - A_{2n}^i \exp(j\beta_{2n}z)]e_{2\rho n} \quad (10a)$$

$$E_{2\phi} = \sum_{n=1}^{N_2} [A_{2n}^r \exp(-j\beta_{2n}z) + A_{2n}^i \exp(j\beta_{2n}z)]e_{2\phi n} \quad (10b)$$

$$H_{2\rho} = \sum_{n=1}^{N_2} [A_{2n}^r \exp(-j\beta_{2n}z) - A_{2n}^i \exp(j\beta_{2n}z)]h_{2\rho n} \quad (10c)$$

$$H_{2\phi} = \sum_{n=1}^{N_2} [A_{2n}^r \exp(-j\beta_{2n}z) + A_{2n}^i \exp(j\beta_{2n}z)]h_{2\phi n} \quad (10d)$$

where expressions for $e_{2\rho n}$, $e_{2\phi n}$, $h_{2\rho n}$, and $h_{2\phi n}$ are given by (4).

Enforcement of the conditions that the tangential-field components must be continuous across the interface ($z = 0$) and application of

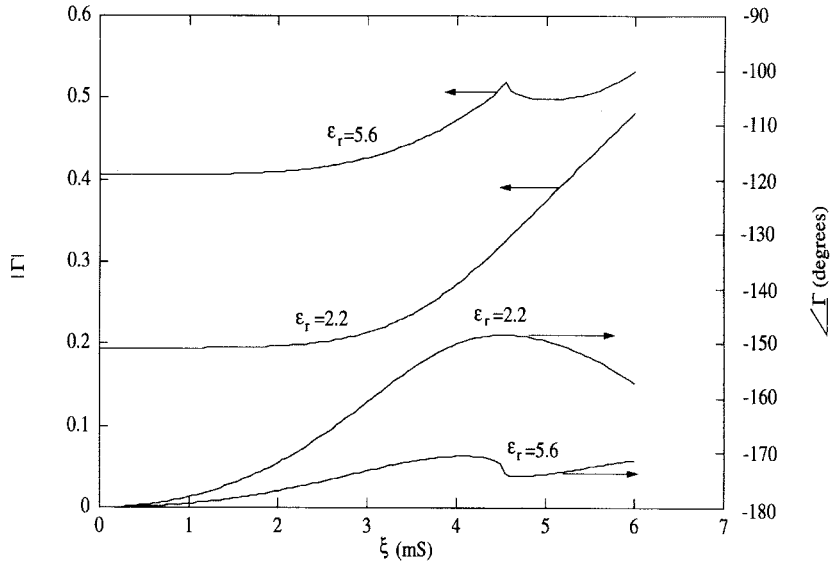

Fig. 3. Magnitude and phase of the reflection coefficient Γ of the dominant TEM mode incident on a nonchiral–chiral interface in a coaxial waveguide ($k_0 r = 0.5$, $R = 3r$, $\epsilon_r = \mu_r = 1$, $\epsilon_{r1} = 1$).

the orthogonality relation (8) for the coaxial Guide II, and (5) for the conventional coaxial Guide I, result in

$$\mathbf{D}(\mathbf{A}_2^r - \mathbf{A}_2^i) = \mathbf{M}_h \mathbf{Y}_1^h (-\mathbf{A}_{1h}^i + \mathbf{A}_{1h}^r) + \mathbf{M}_e (\mathbf{A}_{1e}^i + \mathbf{A}_{1e}^r) \tag{11a}$$

$$\mathbf{A}_{1h}^i + \mathbf{A}_{1h}^r = \mathbf{M}_h^T (\mathbf{A}_2^r + \mathbf{A}_2^i) \tag{11b}$$

$$\mathbf{Y}_1^e (\mathbf{A}_{1e}^i - \mathbf{A}_{1e}^r) = \mathbf{M}_e^T (\mathbf{A}_2^r + \mathbf{A}_2^i) \tag{11c}$$

where $\mathbf{D}$ is a diagonal matrix, the superscript "T" denotes the transpose operation, and $\mathbf{M}_h$ and $\mathbf{M}_e$ are defined as

$$M_{\text{hnm}} = \int_s e_{2\phi n} e_{1\phi m}\, ds \quad M_{\text{enm}} = \int_s h_{2\phi n} e_{1\rho m}\, ds$$

and

$$\mathbf{A}_1 = \begin{bmatrix} \mathbf{A}_{1h} \\ \mathbf{A}_{1e} \end{bmatrix} \quad \mathbf{Y}_1 = \begin{bmatrix} Y_{1h} & 0 \\ 0 & Y_{1e} \end{bmatrix}.$$

From (11), one can derive the following scattering submatrices:

$$\mathbf{S}_{11} = \begin{bmatrix} \mathbf{I} - \mathbf{Y}_{hh} & -\mathbf{Y}_{he} \\ -\mathbf{Y}_{eh} & -(\mathbf{Y}_{ee} + \mathbf{Y}_1^e) \end{bmatrix}^{-1} \begin{bmatrix} -\mathbf{I} - \mathbf{Y}_{hh} & \mathbf{Y}_{he} \\ -\mathbf{Y}_{eh} & (\mathbf{Y}_{ee} - \mathbf{Y}_1^e) \end{bmatrix} \tag{12a}$$

$$\mathbf{S}_{21} = \mathbf{D}^{-1} ([\mathbf{M}_h \mathbf{Y}_1^h \quad \mathbf{M}_e]\, \mathbf{S}_{11} + [-\mathbf{M}_h \mathbf{Y}_1^h \quad \mathbf{M}_e]) \tag{12b}$$

$$\mathbf{S}_{12} = \begin{bmatrix} \mathbf{I} - \mathbf{Y}_{hh} & -\mathbf{Y}_{he} \\ -\mathbf{Y}_{eh} & -(\mathbf{Y}_{ee} + \mathbf{Y}_1^e) \end{bmatrix}^{-1} \begin{bmatrix} \mathbf{M}_h^T \\ \mathbf{M}_e^T \end{bmatrix} \tag{12c}$$

$$\mathbf{S}_{22} = \mathbf{I} + \mathbf{D}^{-1} [\mathbf{M}_h \mathbf{Y}_1^h \quad \mathbf{M}_e]\, \mathbf{S}_{12} \tag{12d}$$

where

$$\begin{aligned} \mathbf{Y}_{hh} &= \mathbf{M}_h^T \mathbf{D}^{-1} \mathbf{M}_h \mathbf{Y}_1^h \\ \mathbf{Y}_{he} &= \mathbf{M}_h^T \mathbf{D}^{-1} \mathbf{M}_e \\ \mathbf{Y}_{eh} &= \mathbf{M}_e^T \mathbf{D}^{-1} \mathbf{M}_h \mathbf{Y}_1^h \\ \mathbf{Y}_{ee} &= \mathbf{M}_e^T \mathbf{D}^{-1} \mathbf{M}_e. \end{aligned}$$

After obtaining the scattering matrix of the dielectric step discontinuity in a coaxial waveguide, we can then confront the problem of a chiral sheath of length t in a coaxial waveguide. The structure illustrated in Fig. 1 can be regarded as a cascaded connection of two junctions and the generalized scattering-matrix technique [10] may be invoked to determine the overall scattering matrix.

IV. Numerical Results

In this section, we present some numerical results for the reflection and transmission coefficients of a wave incident on a nonchiral–chiral interface in a coaxial waveguide. In our computations, the TEM mode is the unique propagating mode in the nonchiral coaxial waveguide.

First, we give some computed results for the first three axisymmetric modes in a coaxial chirowaveguide. The dominant mode of the coaxial chirowaveguide is termed EH_{00}, which corresponds to the TEM mode in a conventional coaxial waveguide; the first two higher order modes are then designated as EH_{01} and HE_{01} corresponding to the modes TM_{01} and TE_{01} in a coaxial line, respectively. The dispersion diagram for these three modes is shown in Fig. 2, where the vertical axis represents $(\beta/k_0)^2$, which gives the relevant information for EH_{01} and HE_{01} when they are cutoff. The cutoff frequency of the dominant EH_{00} mode is zero, while the cutoff frequencies of EH_{01} and HE_{01} modes are, respectively, at about $0.224c/r$ and $0.251c/r$, with c being the velocity of light.

The formulation described in the previous sections and the written computer codes for the scattering matrix of the nonchiral–chiral interface in a coaxial waveguide are verified by considering the reduced case when $\xi = 0$, along with considering power conservation. When $\xi = 0$, the problem considered reduces to a very simple one—a dielectric discontinuity in a coaxial waveguide whose solution is easily obtained. The reflection coefficient of a TEM mode incident on such an interface of two nonchiral dielectrics is $\Gamma = (1 - \sqrt{\epsilon_r/\epsilon_{r1}})/(1 + \sqrt{\epsilon_r/\epsilon_{r1}})$; no higher order modes can be excited by this discontinuity. Our results for the simplified case agree with this analytical solution. The sum of powers of the reflected wave and the transmitted wave is always equal to that of the incident wave within the tolerance of numerical errors.

The magnitude and phase of the refection coefficient of the dominant TEM mode incident on a nonchiral–chiral interface in a coaxial waveguide are shown in Fig. 3 for different permittivities of the chiral material. From Fig. 3, it can be seen that the chirality admittance does have significant influence on the reflection coefficient, both in magnitude and in phase. The effect of the chirality becomes weak when the relative permittivity of the chiral material increases as expected.

Fig. 4 presents the variation of magnitude and phase of the reflection coefficient of a TEM wave incident on a chiral sheath

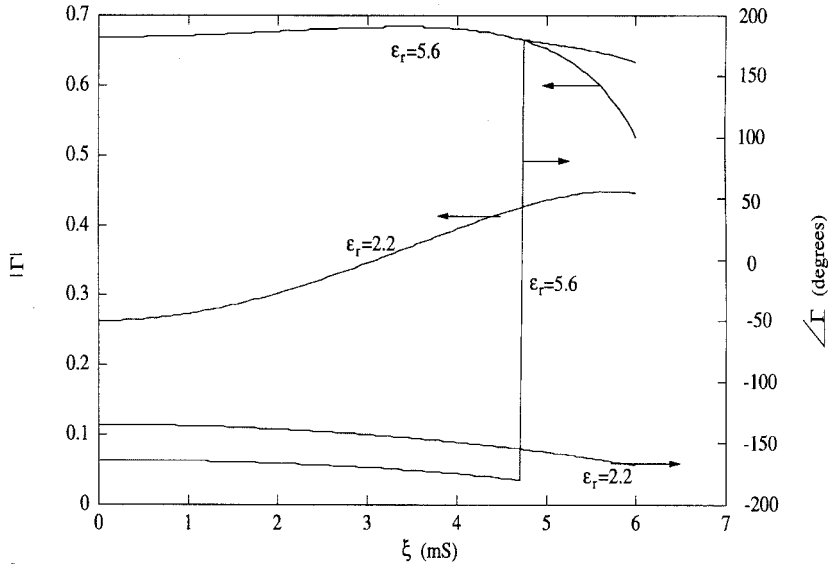

Fig. 4. Magnitude and phase of the reflection coefficient Γ of the dominant TEM mode incident on a chiral sheath in a coaxial waveguide ($k_0 r = 0.5$, $R = 3r$, $\epsilon_r = \mu_r = 1$, $\epsilon_{r1} = 1$, $t = r$).

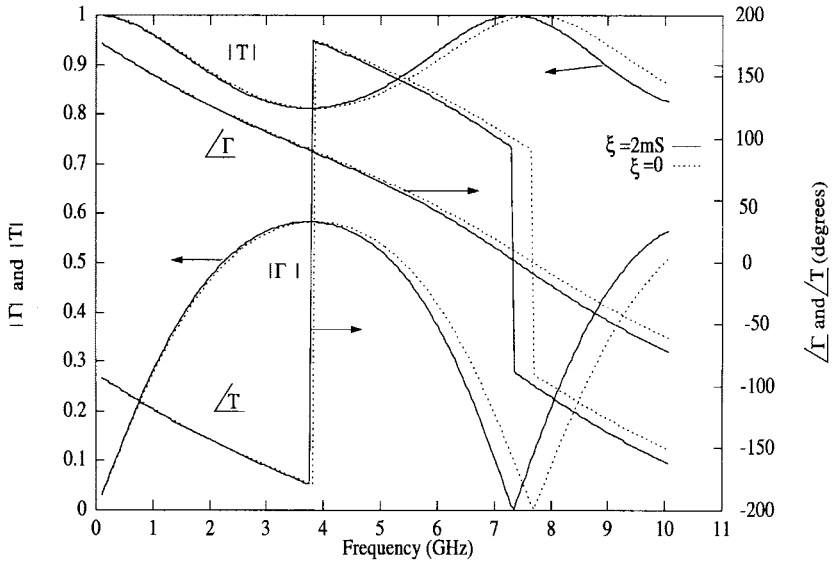

Fig. 5. Frequency characteristics of the reflection and transmission coefficients for a chiral sheath layer of length t in a coaxial waveguide ($r = 1.5$ mm, $R = 3r$, $\epsilon_{r1} = \mu_r = 1$, $t = 10$ mm, $\epsilon_r = 3.8$).

of length t in a coaxial waveguide as functions of the chirality admittance ξ. Both the permittivity and the chirality admittance of the chiral material have an effect on the reflection and transmission coefficients, which implies that one can measure both the relative permittivity and chirality of the chiral material by measuring both the reflection and transmission coefficients simultaneously. The frequency characteristics of the reflection and transmission coefficients of a chiral sheath in a coaxial line are shown in Fig. 5, where the curves for nonchiral ($\xi = 0$) sheath are also plotted for comparison. It is obvious that the effect of the dielectric sheath is negligible when the frequency is very low. When frequency increases, the variation of both the reflection and the transmission-coefficient amplitudes resembles an oscillating curve with no reflection occurring when $t = n\lambda/2$, here n is an integer. The chirality admittance of the material changes the locations of the maxima and minima of the curves.

REFERENCES

[1] N. Engheta and D. L. Jaggard, "Electromagnetic chirality and its applications," *IEEE AP-S Newslett.*, vol. 30, no. 5, pp. 6–12, 1988.

[2] I. V. Lindell *et al.*, *Electromagnetic Wave in Chiral and Bi-Isotropic Media.* Norwood, MA: Artech House, 1994.

[3] F. Mariottee and N. Engheta, "Reflection and transmission of guided electromagnetic wave at an air–chiral interface and a chiral slab in a parallel-plate waveguide," *IEEE Trans. Microwave Theory Tech.*, vol. 41, pp. 1895–1906, Nov. 1993.

[4] P. Pelet and N. Engheta, "The theory of chirowaveguides," *IEEE Trans. Antennas Propagat.*, vol. 38, pp. 90–97, Jan. 1990.

[5] J. A. M. Svedin, "Propagation analysis of chirowaveguides using the finite-element method," *IEEE Trans. Microwave Theory Tech.*, vol. 38, pp. 1488–1496, Oct. 1990.

[6] R. E. Collin, *Field Theory of Guided Waves*, 2nd ed. Piscataway, NJ: IEEE Press, 1991.

[7] N. Engheta and P. Pelet, "Mode orthogonality in chirowaveguides," *IEEE Trans. Microwave Theory Tech.*, vol. 38, pp. 1631–1634, Nov. 1990.

[8] G. Busse and A. F. Jacob, "Complex power and mode coupling in circular chirowaveguide," *IEEE Trans. Microwave Theory Tech.*, vol. 43, pp. 1182–1186, May 1995.
[9] N. Marcuvitz, *Waveguide Handbook.* New York: McGraw-Hill, 1951.
[10] R. Mittra and S. W. Lee, *Analytical Techniques in the Theory of Guided Waves.* New York: Macmillan, 1971.

An Integrated Doppler-Radar Transceiver Front End Using Two FET Active Antennas

Zhengping Ding and Kai Chang

***Abstract*—An integrated X-band Doppler-radar transceiver front end has been developed. This front end consists of two adjacently spaced field-effect transistor (FET) active antennas, with one of them being biased to oscillate as its transmitter and the other being biased not to oscillate, but to act as its mixer. This design has the advantage of lower noise at low Doppler frequencies as compared to a self-oscillating mixer scheme. The circuit can be used in low-power Doppler-radar systems to detect slow-moving objects such as pedestrians, intruders, automobiles, etc., with high sensitivity.**

***Index Terms*— Active antennas, Doppler radar, integrated antennas, transceivers.**

I. Introduction

In recent years, efforts have been made in searching for appropriate active antenna designs for seemingly promising spatial power-combining technology [1]–[6]. Mixers built directly on antennas have also been reported [7], [8]. These innovations are very attractive in realizing compact radio-frequency (RF) front ends in portable communications and radar systems. Active antennas used for communications have been reported in literature [9]. On the other hand, active antennas used for radar systems have not been paid sufficient attention.

To probe into potential applications of active antennas in low-power Doppler-radar systems, a compact X-band Doppler-radar transceiver front end was built and tested. In this design, two field-effect transistor (FET) active antennas were adjacently integrated on one substrate. One FET active antenna is biased to oscillate and radiate as the transmitter, while the other is biased not to oscillate, but to serve as the mixer/receiver. The local oscillator (LO) signal of the mixer is from the oscillating active antenna via mutual coupling. The RF signal is reflected from any moving object in the beam of the active antennas. Compared to the self-oscillating mixer scheme, this design demonstrated much lower noise at low Doppler frequencies ranging from hertz to kilohertz order. Therefore, it can be used in Doppler-radar applications for the detection of slow-moving objects.

II. Circuit Design and Operation

The integrated RF front end was fabricated with two Hewlett-Packard ATF-26 836 FET's on an RT/Duroid 5880 dielectric substrate of $\varepsilon_r = 2.20$ and thickness $h = 0.787$ mm, as shown in Fig. 1. The design frequency was chosen at 10 GHz. The design of the FET active antenna is similar to the one reported earlier with Gunn diodes [6]. The active antenna uses a ring stabilized FET oscillator coupled to a slot antenna. The bias circuits and FET's are hidden behind the metallization. This active antenna design has the advantages of low spurious radiation, low cross polarization, ease of integration, etc. The circumference of the 67-Ω microstrip ring resonator was designed such that their first resonance is at the design frequency. The length of the 0.5-mm-wide slot antenna was designed such that their first resonance is also at the design frequency. The reason that the first resonance of the microstrip ring and the slot antenna was designed to be at the same frequency is to avoid possible mode-jumping phenomena due to multiple resonance of the circuits [10]. The drains of the FET's were connected to the resonant microstrip rings. Their sources were grounded through via holes. Their gates were terminated with an RF reactance X_t, which was realized by an open-circuited microstrip stub. Both FET active antennas were designed identically. One FET active antenna (FET 1) was biased to oscillate/radiate, while the other (FET 2) to mix/receive. The two FET active antennas are closely spaced such that certain LO power can be coupled from the oscillating/radiating active antenna to the mixing one. This makes the pair of active antennas a monostatic Doppler-radar transceiver front end. Doppler signals are extracted from the drain of the FET in the mixer/receiver circuit. A shield plate was introduced a certain distance behind the circuits to avoid any back radiation.

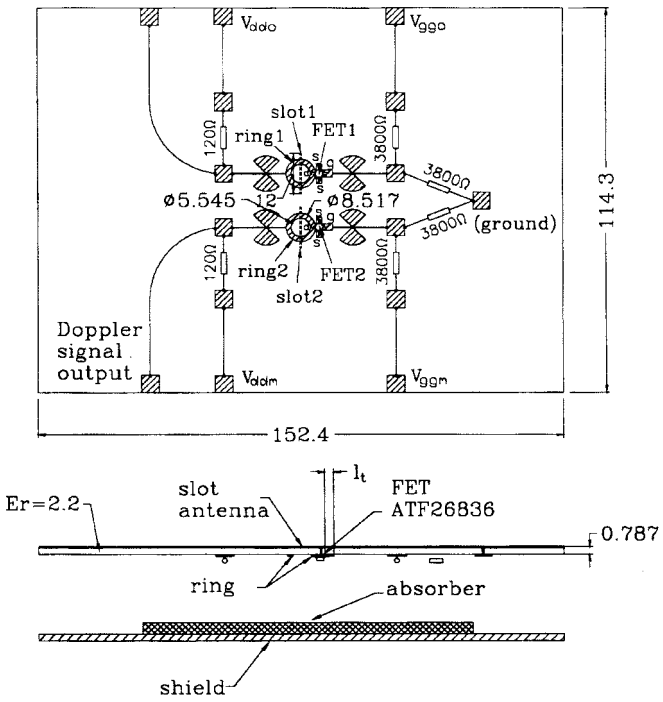

Fig. 1. Circuit design (all dimensions are in millimeters).

The dimensions of the 67-Ω microstrip ring and the 0.5-mm-wide slot antenna were determined by means of EEsof's LineCalc software. The dimensions of the open-circuited microstrip stub in the circuit was determined by means of the small-signal approach for the design of the FET oscillators [11].

Fig. 2 shows the schematic equivalent circuits of this active antenna, including both the oscillator/transmitter circuit and the

Manuscript received May 14, 1996; revised April 7, 1998.

The authors are with the Department of Electrical Engineering, Texas A&M University, College Station, TX 77843-3128 USA (e-mail: chang@eesun1.tamu.edu).

Publisher Item Identifier S 0018-9480(98)04948-5.